ELSEVIER

Journal of Magnetism and Magnetic Materials 233 (2001) 169–180

Journal of magnetism and magnetic materials

www.elsevier.com/locate/jmmm

Phase stability and site preference of $Sm(Fe,T)_{12}$

Chen Nan-xian[a,*], Hao Shi-qiang[b], Wu Yu[b], Shen Jiang[b]

[a] *Department of Physics, Tsinghua University, Beijing 100084, China*
[b] *Institute of Physics, University of Science and Technology, Beijing 100084, China*

Received 18 October 2000; received in revised form 12 January 2001

Abstract

The structure of intermetallics $Sm(Fe,T)_{12}$ is analyzed via a quasi-ab initio pair potentials $\Phi_{Fe-Fe}(r)$, $\Phi_{Sm-Fe}(r)$, $\Phi_{Sm-Sm}(r)$, $\Phi_{Sm-T}(r)$, $\Phi_{Fe-T}(r)$ and $\Phi_{T-T}(r)$. The calculation results show that each of Cr, V, Mo and Ti significantly decreases the cohesive energy of $Sm(Fe,T)_{12}$, and thus stabilizes its structure of $ThMn_{12}$. The calculated lattice constants coincide quite well with experimental values. The sequence of site preference occupation is 8i, 8j and 8f, with the 8i occupation corresponding to the greatest energy decrease. The calculated results also show that each of Co, Cu, Ni and Sc does not stabilize the system with the structure of $ThMn_{12}$. The calculated crystal structure can recover after either an overall wide-range macro-deformation or atomic random motion, demonstrating that an Sm–Fe–T system has the stable structure of $ThMn_{12}$. The crystal space group remaining consistent at different temperatures is also shown in this paper. All of the results verify that the first principle potentials based on the lattice inversion technique are effective.

PACS: 81.05.zx; 61.66. − f; 61.18. − j; 64.70. − p

Keywords: Structure determination; Site preference; Interatomic potentials; Phase stability; Lattice inversion

1. Introduction

In 1981, Yang and his colleagues found that the structure of intermetallics $Y(Mn_{1-x}Fe_x)_{12}$ is of $ThMn_{12}$ [1]. In 1987, Mooij found that the structure of the iron-based compound $RFe_{10}V_2$ is also of $ThMn_{12}$. Since then, many compounds with the same structure have been found [2,3]. These compounds have high Curie temperatures and high magnetic moments, valuable for practical applications. Actually, the binary compound RFe_{12} is metastable, but as a small amount of ternary element T (T = Cr, Mo, V, Ti) is added, $Sm(Fe,T)_{12}$ is stable. The crystal cell of RFe_{12} is shown in Fig. 1. Its space group is I4/mmm, with two formula units (26 atoms) included. There are four crystal sites: 2a, 8i, 8j and 8f. The rare-earth atoms occupy the 2a site and the Fe atoms occupy 8i, 8j and 8f sites. According to the neutron diffraction, most stabilizing element T (such as V and Ti) atoms preferentially substitute Fe atoms [4–8].

In this paper, the interatomic pair potentials obtained by lattice inversion are used to analyze the phase stability and site preference substitution of $Sm(Fe,T)_{12}$, where T is either a 3d or 4d

*Corresponding author. Tel.: +86-10-623-23577; fax: +86-10-623-27283.

E-mail address: nanxian@hotmail.com (C. Nan-xian).

0304-8853/01/$ - see front matter
PII: S0304-8853(01)00251-7

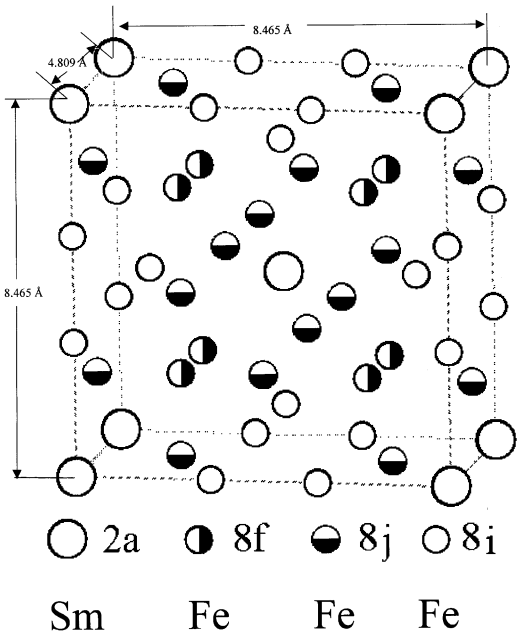

Fig. 1. The crystal cell of $SmFe_{12}$ with two formula units.

element. The calculated total energy is used as the criterion for studying the stability and site preference occupation. For the 3d elements, the calculation results coincide quite well with the experimental data. For the 4d elements, the calculation results are considered as a prediction of the stability and site preference occupation. In the second part of this paper the calculation algorithm is described. The comparison of the calculated results with the experimental data is shown in Section 3. A concise qualitative analysis for the calculated results is demonstrated in the fourth part, and the fifth part is the conclusion and discussion.

2. Calculation algorithm

In general, any interatomic pair potential can be obtained by a strict lattice inversion of cohesive energy curves, and the cohesive energy curves can be obtained either by a first principle calculation or experimental data fitting. In this part, we focus on the lattice inversion theorem.

2.1. Lattice inversion theorem

Here we take a single element crystal, for example, to explain how to use Chen's lattice inversion theorem to obtain the interatomic pair potential from a first principle cohesive energy curve [9–14].

Suppose that the crystal cohesive energy obtained by the first principle calculation can be expressed as

$$E(x) = \frac{1}{2}\sum_{n=1}^{\infty} r_0(n)\Phi(b_0(n)x), \tag{1}$$

where x is the nearest-neighbor distance, $r_0(n)$ is the nth neighbor coordination number, $b_0(n)x$ is the distance between the reference central atom and its nth neighbor, and $\Phi(x)$ is the pair potential. By a self-multiplicative process from $\{b_0(n)\}$, the $\{b(n)\}$ is formed, a multiplicative closed semigroup. This implies that a lot of virtual lattice points are involved, but the corresponding virtual coordination number is zero. In the $\{b(n)\}$, for any two integers m and n, there is a sole integer k such that $b(k) = b(m)b(n)$. Hence, Eq. (1) can be rewritten as

$$E(x) = \frac{1}{2}\sum_{n=1}^{\infty} r(n)\Phi(b(n)x), \tag{2}$$

where

$$r(n) = \begin{cases} r_0\left(b_0^{-1}[b(n)]\right) & \text{if} \quad b(n) \in \{b_0(n)\}, \\ 0 & \text{if} \quad b(n) \notin \{b_0(n)\}. \end{cases} \tag{3}$$

Then the general equation for the interatomic pair potential obtained from the inversion can be expressed as

$$\Phi(x) = 2\sum_{n=1}^{\infty} I(n)E(b(n)x), \tag{4}$$

where $I(n)$ has the characteristics of

$$\sum_{b(d)1b(n)} I(d)r\left(b^{-1}\left[\frac{b(n)}{b(d)}\right]\right) = \delta_{n1}. \tag{5}$$

$I(n)$ is uniquely determined by a crystal geometrical structure, not related to the concrete element category. Thus, the interatomic pair potentials can be obtained from the known cohesive energy function $E(x)$.

The interatomic pair potential between distinct atoms can be obtained similarly by the same inversion method, and they are used to study the rare-earth intermetallics structures. Several relevant interatomic pair potentials are shown in Fig. 2.

2.2. Method for obtaining quasi-ab initio cohesive energy curve

In the present work, the phase stability, site preference, lattice parameter and space group for a series Fe-based rare-earth compounds $Sm(Fe,T)_{12}$ are evaluated by using quasi-ab initio interatomic pair potentials.

With a conventional method, the ab initio calculation of the cohesive energy curves for $Sm(Fe,T)_{12}$ is impossible or very difficult. The reason is not only due to the structural complexity of ternary alloys $SmFe_{12-x}T_x$, but also due to the divergence occurring in the total energy calculation. In order to find some effective interatomic potentials with the number-theoretic lattice inversion technique, a practical method of performing the ab initio calculation of cohesion curve is needed. For this, the search and design of some simple and virtual structures covering the necessary interatomic potentials are important for us. For example, in order to obtain potentials $\Phi_{Fe-Fe}(x)$, $\Phi_{Sm-Sm}(x)$ and $\Phi_{Sm-Fe}(x)$, we designed three structures, respectively, as follows.

First, let us consider the structure of BCC Fe as B_2 or CsCl structure with two simple cubic sublattices Fe_1 and Fe_2. Thus, we calculate

$$\begin{aligned} E(x) &= E_{Fe}^{BCC}(x) - E_{Fe_1}^{SC}(x) - E_{Fe_2}^{SC}(x) \\ &= \sum_{i,j,k\neq 0}^{\infty} \Phi_{Fe-Fe} \\ &\quad \times \left(\sqrt{\tfrac{4}{3}\left[\left(i-\tfrac{1}{2}\right)^2 + \left(j-\tfrac{1}{2}\right)^2 + \left(k-\tfrac{1}{2}\right)^2 \right]} x \right), \end{aligned}$$

where x is the nearest-neighbor distance in the BCC structure, $E_{Fe}(x)$ represents the total energy curve with a BCC structure, $E_{Fe1}(x)$ or $E_{Fe2}(x)$ is the total energy function with a simple cubic structure. Now, $E(x)$ automatically becomes the cohesive energy function of one Fe_1 atom with all the Fe_2 atoms. Here, the Fe_2 atoms form a simple cubic structure, and only one Fe_1 atom is located at the center of any one cube. Then the $\Phi_{Fe-Fe}(x)$ can be obtained directly by using Chen's lattice inversion technique.

Similarly let us consider the Sm with FCC structure as $L1_2$ structure, it is given

$$E(x) = E_{Sm}^{FCC}(x) - E_{Sm}^{SC}(x) - E'_{Sm}(x),$$

where $E_{Sm}^{SC}(x)$ is attributed to the simple cubic structure, in which all the atoms occupy the corner sites and $E'_{Sm}(x)$ is attributed to the atoms occupying the face center sites. Thus, the $\Phi_{Sm-Fe}(x)$ can also be obtained by Chen's lattice inversion technique.

The ab initio calculation of the total energy curve related to $\Phi_{Sm-Fe}(x)$ is very hard to perform. We find that the calculation for Sm_3Fe with $L1_2$ structure can be done in a nearly equilibrium position, and this gives simply the three parameters for the cohesion function under Morse approximation or Rose approximation.

From the above, all the quasi-ab initio interatomic potentials are given and shown in Fig. 2. Note that again in the above procedure, the total energy has been reduced to the cohesive energy.

By using these quasi-ab initio interatomic potentials from some simple virtual structures, the cohesive energy for much complex structures can be obtained directly even though some foreign additions are involved.

By using the above quasi-ab initio interatomic potentials, a large number of calculations for phase stability, site preference, lattice parameters and tolerance range have been performed with unexpectedly good agreement with the experiment for these structural properties.

This indicates that the pair potentials based on some simple ab initio calculation and lattice inverse formula can evaluate some structural properties for quite complex Fe-based rare-earth intermetallics.

3. Calculation results

In this paper, we take 14 Å as the cut-off radius. Energy minimization is carried out using a

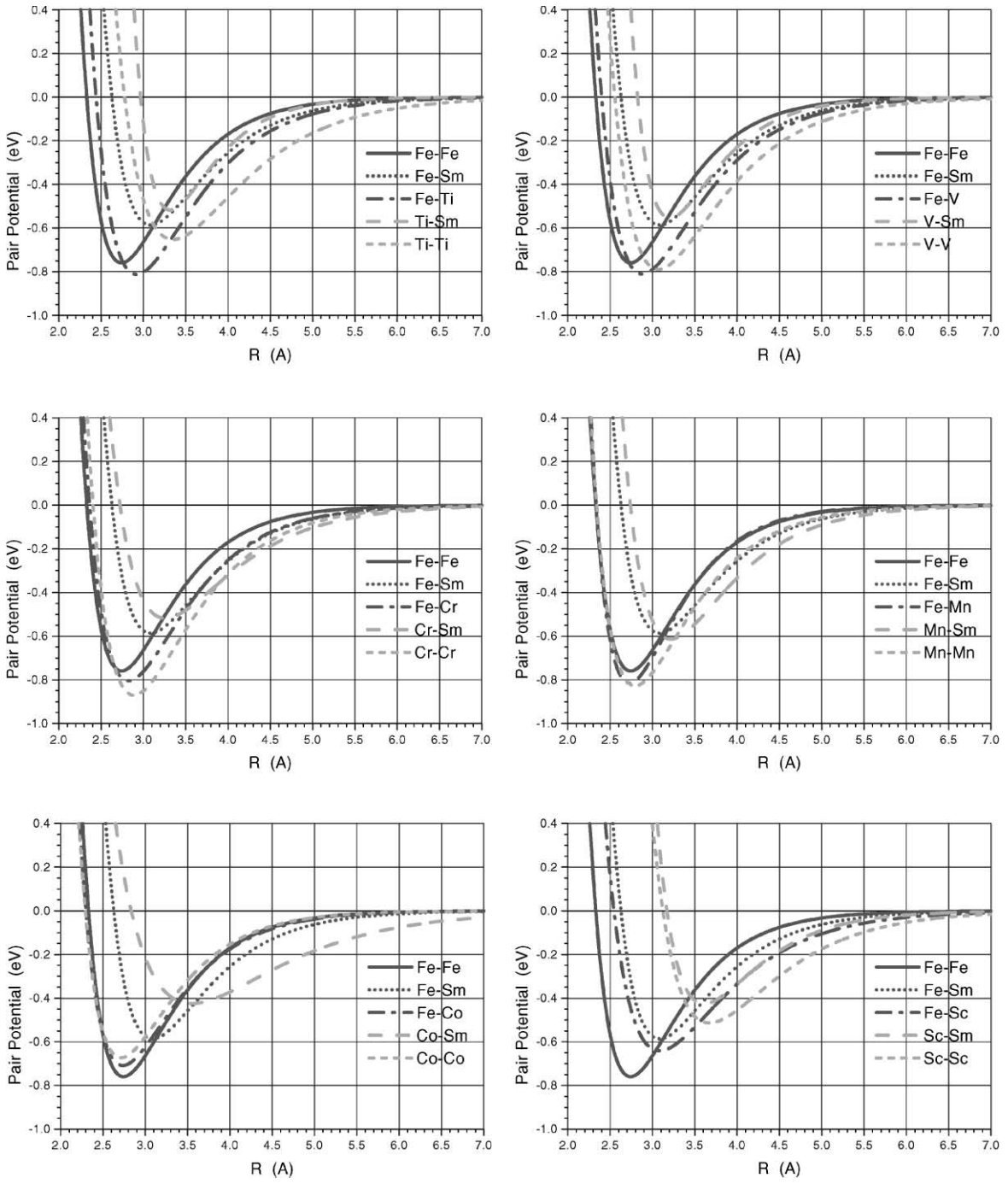

Fig. 2. Some important interatomic potentials.

conjugate gradient method. In order to reduce statistical fluctuation, we take the periodical cell containing 208 atoms, $(RFe_{12-x}T_x)_{16}$, for simulation.

3.1. Calculation of structural parameters

3.1.1. $SmFe_{12}$ binary metastable structure

Despite the structure of $SmFe_{12}$ being metastable, it can be considered as the eigen-structure of $Sm(Fe,T)_{12}$. In the calculation procedure, the initial lattice constants of $SmFe_{12}$ are randomly chosen in a certain range. Under the control of the interatomic pair potentials, the energy minimization is carried out. The results show that in the range of 0.001–0.5 Å, the space group maintains I4/mmm, the atomic site occupation is similar to that of $ThMn_{12}$, and the lattice constants after stabilization are $a = 8.465$ Å, $c = 4.809$ Å, $\alpha = \beta = \gamma = 90^\circ$ (Table 1). A certain range randomness of the initial structure and the stability of the final structure illustrate that the $SmFe_{12}$ has a topological invariability with respect to the stably existing $Sm(Fe,T)_{12}$. It also furnishes convincing evidence that the interatomic pair potentials are reliable for the study of material structural characteristics.

3.1.2. Ternary system $Sm(Fe,T)_{12}$

Substitute the atoms of ternary element T (T = Cr, Mo, Ti, and V) for the randomly chosen Fe atoms at a certain lattice site, and then make the lattice relaxation. From the dependence of the lattice constant on the additional content of the ternary element (Fig. 3), one can see that the changes of lattice constant are relatively small if the T atoms occupy 8i sites, and the changes of lattice constant are relatively big if the T atoms occupy 8j and 8f sites. It is noteworthy that we neglect in the calculation the coexistence of two phases. The calculated lattice constants are compared with the experimental values, as shown in Table 2.

3.2. Phase stability and site preference substitution

3.2.1. The phase stability of $Sm(Fe,T)_{12}$

The substitution of T atoms for Fe atoms causes a cohesive energy change, and different contents of T cause different amounts of cohesive energy change. The relation between the crystal cohesive energy and the added ternary element content are shown in Fig. 4. It can be seen that if T is Cr, Mo, Ti or V, the cohesive energy decreases, illustrating that each of these elements can stabilize the crystal and that the stabilized phases exist. (The total energies of the intermetallics shown in the figure are the statistical average of 20 samples, the symbol 'I' indicates the range of mean square root error.) The total energy decline of the intermetallics containing Mo is more evident than that of the intermetallics containing Ti. This means that the solubility of Mo is higher, in agreement with experiments [4,5]. Additionally, the substitution

Table 1
Crystal constants of $SmFe_{12}$

Initial state						Final state					
a (Å)	b (Å)	c (Å)	α	β	γ	a (Å)	b (Å)	c (Å)	α	β	γ
2	2	2	90°	90°	90°	8.464	8.464	4.81	90°	90°	90°
2	2.5	3	95°	85°	90°	8.465	8.465	4.809	90°	90°	90°
12	12	12	90°	90°	90°	8.465	8.465	4.809	90°	90°	90°
8	8	5	60°	60°	60°	8.465	8.465	4.809	90°	90°	90°
16	16	10	90°	90°	90°	8.465	8.465	4.809	90°	90°	90°
2	2	2	80°	80°	80°	8.465	8.465	4.809	90°	90°	90°
10	10	10	88°	88°	88°	8.465	8.465	4.809	90°	90°	90°
2	2	2	50°	50°	50°	4.810	8.465	8.465	90.01°	90°	90°
20	20	10	70°	80°	60°	9.736	9.736	4.810	60.4°	60.39°	75.87°

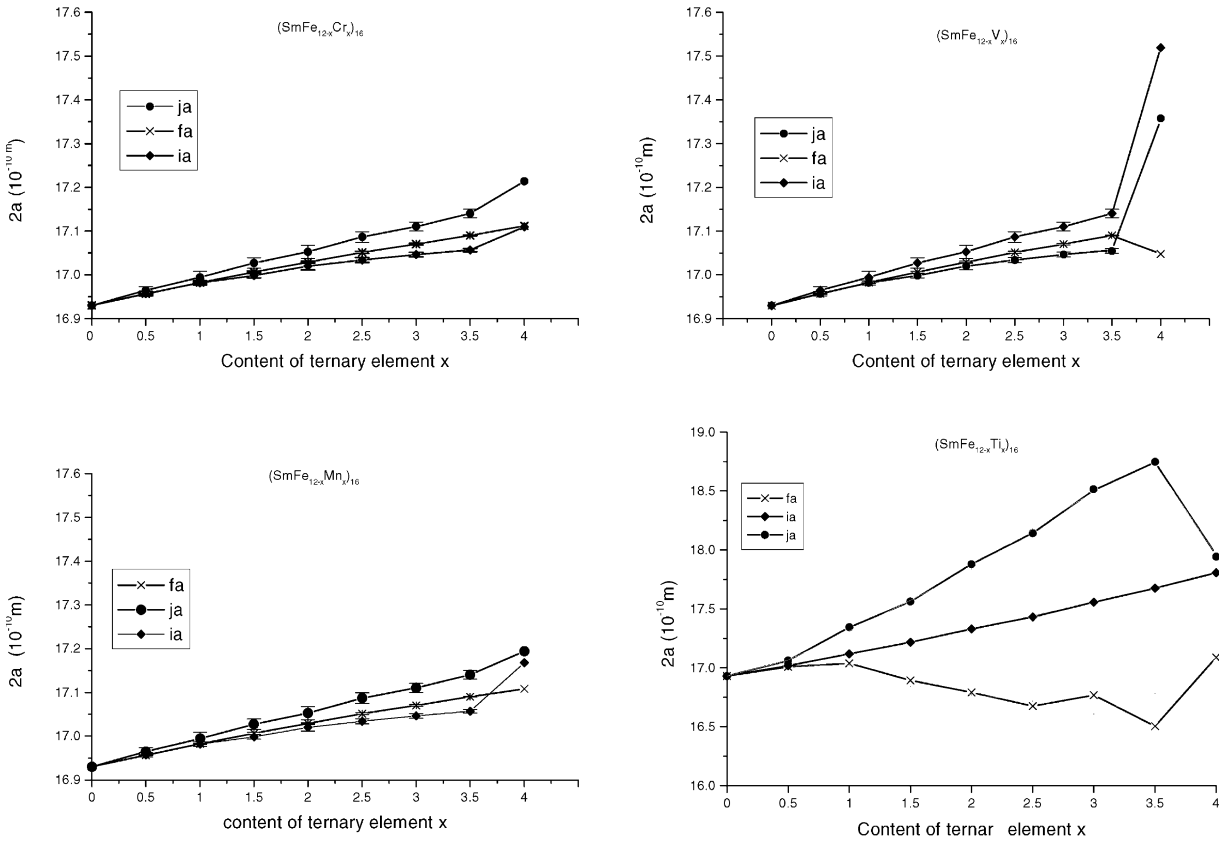

Fig. 3. Dependence of the lattice constant on the content of ternary additions.

Table 2
Comparison of calculated and experimental lattice constants

	Calcul. a (Å)	Exp. a (Å)	Calcul. c (Å)	Exp. c (Å)
$SmFe_{12}$	8.465	—	4.809	—
$SmFe_{10}Cr_2$	8.504	8.496	4.821	4.7599 [4]
$SmFe_{10}V_2$	8.6	8.5368	4.838	4.7722 [4]
$SmFe_{11}Ti$	8.658	8.576	4.872	4.800 [15]
$SmFe_{10}Mo_2$	8.647	8.59	4.866	4.804 [6]

behaviors of other 3d and 4d elements are also studied. For example, if T = Ni, Cu, Co, Sc or Zn, the cohesive energy of $Sm(Fe,T)_{12}$ increases, it means that these elements cannot stabilize the $SmFe_{12}$ system with the structure of $ThMn_{12}$.

3.2.2. Site preference substitution

It is shown in Fig. 4 that the calculated cohesive energy decreases most significantly while T atoms preferentially occupy 8i sites, the energy decreases less significantly if T atoms occupy 8j sites, and even less corresponding to 8f sites. Therefore, the T atoms preferentially occupy 8i sites, in good agreement with experiments [4–8]. Some of the experiments assert that Ti atoms occupy not only 8i but also 8j sites. But from the calculation results, we find that the cohesive energy difference is not negligible comparing the cases of Ti atoms

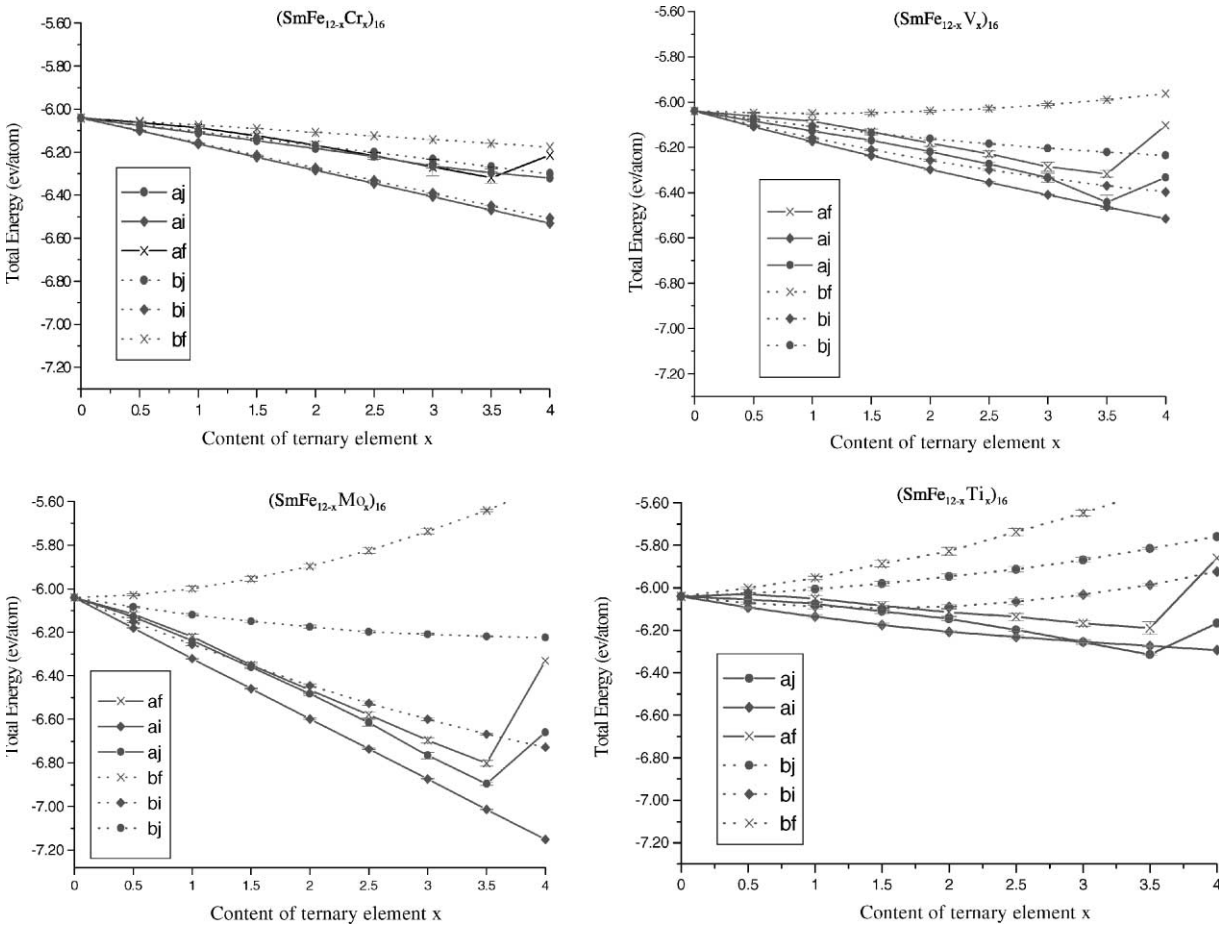

Fig. 4. Site preference of T = Cr, V, Mo and Ti, in $SmFe_{12}$ and phase stability.

occupying 8i sites and occupying 8j sites. The statement that Ti atoms occupy 8i and 8j sites simultaneously could not be explained.

When T = Mn, the energy changes with increasing content x, forming a convex curve. That means as the content is small, the energy increases with the increasing content, but as the content is big enough, the total energy decreases significantly with the increasing content, illustrating that as the content x increases $SmFe_{12-x}Mn_x$ becomes more stable and accordingly there should be a stable $SmMn_{12}$. In other words, the structure of RMn_{12} is more stable than that of RFe_{12} (Fig. 5).

3.3. The relationship between the tolerance and the $Sm(Fe,V)_{12}$ structure

3.3.1. The stability of $Sm(Fe,V)_{12}$ structure with respect to the atomic random motion

Let T = V and substitute the V atoms for a randomly selected part of Fe atoms at the 8i sites, thus forming the $(SmFe_{10}V_2)_{16}$. Then make use of the conjugate gradient method to minimize the system energy, as an approximation of a practical relaxation process. The results show that the space group is I4/mmm within the range of 0.15–1.00 Å.

If the atoms in the $(SmFe_{10}V_2)_{16}$ crystal cell move randomly in a certain range, then using the

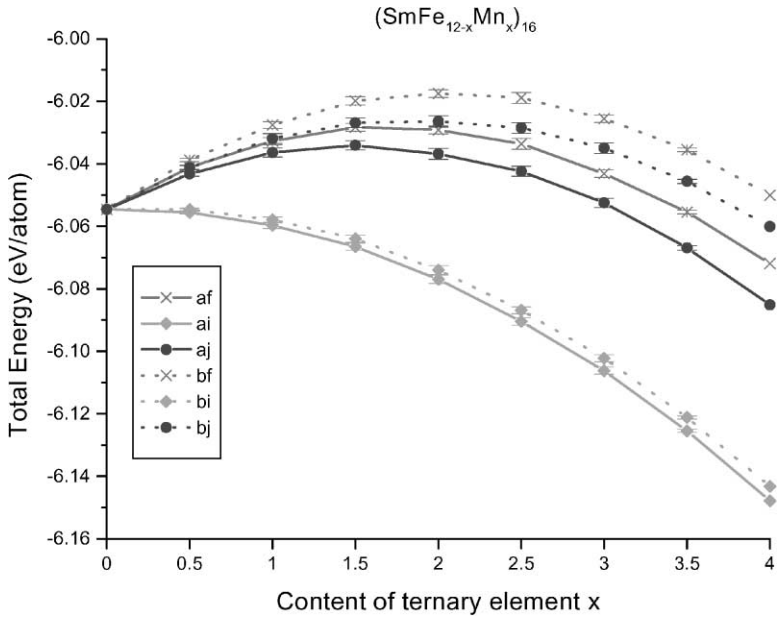

Fig. 5. The cohesive energy curve of $SmFe_{12-x}Mn_x$.

conjugate gradient for relaxation, the result shows that the lattice constants are in good agreement with the experimental data, still retaing $a = 8.465\,\text{Å}$, $b = 8.465\,\text{Å}$, $c = 4.809\,\text{Å}$, $\alpha = \beta = \gamma = 90^\circ$. If the atomic random motion is within the range of 0.6 Å, the space group can stay in I4/mmm with the tolerance properly increased. If the atomic motion exceeds that range, the space symmetry of the system will drop (Table 3). Thus, the stability of the lattice and the effectiveness of the interatomic pair potentials are verified by the overall wide-range macro-deformation and the atomic random micro-motion.

The structure of $Sm(Fe,V)_{12}$ can recover after either overall wide-range macro-deformation or atomic random micro-motion, demonstrating that the structure is stable. Yet the calculated results show that the allowable macro-structural alternation is greater than the allowable micro-structural alternation. This is because the former is conducted only in a few dimensions in the phase space and the latter in numerous dimensions.

It is worth noting that Table 3 is the statistical results of a few samples.

3.3.2. The structural stability of $Sm(Fe,V)_{12}$ at different temperatures

The relation between the tolerance and the space group is further studied at higher temperatures. The molecular dynamics NPT ensemble is used, with $P = 1$ atm, $t = 0.001$ ps. The dynamic simulation for $(SmFe_{10}V_2)_{16}$ is carried out at temperatures of 300, 500, 700, 900 and 1200 K. After reaching equilibrium, the symmetry can also remain I4/mmm in a certain range, and the lattice constants change very little with respect to the change in temperature. Thus, the structural stability is again verified. The minimum value of the tolerance for retaining the space group I4/mmm is 0.152 Å. This is the average value of 4 random samples at 300 K. The corresponding mean square root displacement is 0.1414 Å, approximately equal to the tolerance value. The other temperatures calculated results (Table 4) show that each minimum tolerance value all approximately equals to the corresponding mean square root displacement (MSRD). These results further verify that the above calculations are self-consistent and reasonable. The comparisons of

Table 3
After the atomic random motion, the relation between the tolerance and the space group of $Sm(Fe,V)_{12}$

Range of motion	Tolerance range	Space group
0.1 Å	(0.001–0.124)	P1
	(0.125–0.135)	P4/mmm
	(0.136–0.5)	I4/mmm
0.2 Å	(0.001–0.12)	P1
	0.13	P4/mmm
	(0.14–0.5)	I4/mmm
0.3 Å	(0.001–0.12)	P1
	0.13	Cmmm
	(0.14–0.5)	I4/mmm
0.4 Å	(0.001–0.11)	P1
	(0.111–0.118)	Pm
	(0.119–0.125)	P2/m
	(0.14–0.142)	C2/m
	(0.143–0.5)	I4/mmm
0.5 Å	(0.001–0.138)	P1
	0.139	Cmmm
	(0.14–0.142)	P2/m
	(0.143–0.5)	I4/mmm
0.6 Å	(0.001–0.124)	P1
	0.125	Pma2
	(0.127–0.128)	P2/m
	(0.129–0.131)	P222
	(0.132–0.161)	Pmmm
	(0.162–0.164)	P21/m
	(0.165–0.5)	I4/mmm
0.61 Å	(0.001–0.5)	P1

potential energy, kinetic energy and the fluctuation at different temperatures are shown in Table 5.

It can be seen that the potential energy, kinetic energy and total energy as well as the fluctuations all increase with the increasing temperature, yet the fluctuations are small compared to the absolute potential energy values; therefore, the crystal structure at different temperatures is basically determined by the interatomic pair potentials, rarely related to the temperature.

4. Analysis

4.1. Phase stability

The following is the analysis from the point of view of interatomic pair potential. When a small amount of ternary element atoms substitute the Fe atoms, the ternary element atom is surrounded mostly by Fe atoms, and none of the nearest neighbor of Sm are Sm atoms, and none of the nearest neighbors of T are T atoms. Thereby, the pair potentials of $\Phi_{Sm-Sm}(r)$ and $\Phi_{T-T}(r)$ have little influence on the substitution behavior and the structural stability. The energy difference caused by the substitution is mainly determined by the difference between $\Phi_{Fe-T}(r)$ and $\Phi_{Fe-Fe}(r)$. If $\Phi_{Fe-T}(r) < \Phi_{Fe-Fe}(r)$, the T element can stabilize the structure. On the contrary, if $\Phi_{Fe-T}(r) > \Phi_{Fe-Fe}(r)$, then the T element cannot stabilize the structure. Therefore, V, Ti, Cr, Mo,

Table 4
The relationship between tolerance and the space group of $Sm(Fe,V)_{12}$ and MSD at difference temperature

T (K)	Crystal constants			Tolerance range (Å)	Space group	MSD (Å^2/atom)	MSRD (Å/atom)
300	8.465 Å	8.464 Å	4.81 Å	(0.16–0.5)	I4/mmm	0.02	0.1414
	89.99°	89.99°	90°				
500	8.466 Å	8.465 Å	4.809 Å	(0.2–0.5)	I4/mmm	0.03	0.1732
	90°	90°	89.99°				
700	8.466 Å	8.465 Å	4.81 Å	(0.225–0.5)	I4/mmm	0.04	0.2
	89.99°	89.99°	90°				
900	8.465 Å	8.463 Å	4.809 Å	(0.273–0.5)	I4/mmm	0.06	0.245
	89.99°	90°	90.01°				
1200	8.463 Å	8.465 Å	4.81 Å	(0.326–0.5)	I4/mmm	0.07	0.265
	89.99°	89.99°	90°				

Table 5
The potential and kinetic energies and their fluctuations[a]

Energy T	300 K	500 K	700 K	900 K	1200 K
E_P (eV/atom)	− 6.2711	− 6.254	− 6.2176	− 6.1874	− 6.1474
	(0.0004)	(0.0009)	(0.0016)	(0.0025)	(0.003)
E_K (eV/atom)	0.0387	0.0646	0.0907	0.1152	0.1530
	(0.0006)	(0.001)	(0.0015)	(0.0023)	(0.003)
E_T (eV/atom)	− 6.2321	− 6.1809	− 6.1268	− 6.0743	− 5.9948
	(0.00008)	(0.0003)	(0.0008)	(0.0007)	(0.001)

[a] Values in brackets corresponding to energy fluctuations at difference temperature.

Zr and Nb play the role of stabilization, but Ni, Co, Zn and Sc do not play the role of stabilization.

When the amount of the ternary element increases, the possibility of the T atoms getting close to T atoms or rare-earth atoms increases. Then the comparison between $[\Phi_{Sm-Fe}(r) - \Phi_{Sm-T}(r)]$ and $[\Phi_{Fe-Fe}(r) - \Phi_{T-T}(r)]$ has to be made. We found from Fig. 2 that when T = Cr, V or Ti, $\Phi_{Fe-Fe}(r)$ and $\Phi_{T-T}(r)$ are equivalent in the sense of decreasing the total energy, but $\Phi_{Sm-Fe}(r) < \Phi_{Sm-T}(r)$. That means a big amount of the ternary element substitution will cause the total energy to increase, and thereby cause a structural instability. Hence, the solubility of the ternary element is limited.

When T = Mn, although $\Phi_{Sm-Fe}(r) < \Phi_{Sm-T}(r)$, but in the range of 2.3 Å $< r <$ 5.5 Å, not only $\Phi_{Mn-Fe}(r) < \Phi_{Fe-Fe}(r)$ but the $[\Phi_{Mn-Mn}(r) < \Phi_{Fe-Fe}(r)]$ is more significant. Thus, $[\Phi_{Sm-Fe}(r) < \Phi_{Sm-T}(r)]$ no longer plays the deciding role. That means even if there are a lot of Mn atoms, the total energy after the substitution is still lower than that before the substitution. Thus, for $(SmFe_{12-x}Mn_x)_{16}$ the convex shape of the energy vs. ternary element content curve in Fig. 5 can be explained. Compared to $SmFe_{12}$, the structure of is are much more stable.

The above analysis explains why some element can stabilize the binary structure and some do not have such kind of function. Yet in the practical calculation, the results are determined by the relaxation while all of the interatomic pair potentials $\Phi_{Fe-Fe}(r)$, $\Phi_{Sm-Fe}(r)$, $\Phi_{Sm-Sm}(r)$, $\Phi_{Sm-T}(r)$,$\Phi_{Fe-T}(r)$, $\Phi_{T-T}(r)$ are considered simultaneously.

4.2. Site preference substitution

The substitution behavior of the stabilizing atoms can also be explained by the analysis and comparison of interatomic pair potentials. Focusing on the range of 2.3 Å < r < 4.4 Å, note that $\Phi_{Fe-T}(r)$, (T = Cr, Ti, V, and Mo) intercepts with $\Phi_{Fe-Fe}(r)$ at about $r = 2.7$ Å. When the interatomic distance $r < 2.7$ Å, $\Phi_{Fe-T}(r) > \Phi_{Fe-Fe}(r)$, so that it is unfavorable for the substitution of T atoms for the Fe atoms, and when the distance $r > 2.7$ Å, $\Phi_{Fe-T}(r) < \Phi_{Fe-Fe}(r)$, it is favorable for the substitution.

In the range of 2.3 Å $< r <$ 4.4 Å, $\Phi_{Sm-T}(r)$ is higher than other pair potentials, if the T (T = Cr, Ti, V, etc.) atoms occupy 8i sites which are more distant from the Sm atom, then it is energy favorable. If the T atoms occupy 8j or 8f sites, the $\Phi_{Sm-T}(r)$ is greater, energy unfavorable.

The site preference occupation of the ternary atoms may also be analyzed by the affecting factors as shown in Table 6.

The first column in the Table includes the sites occupied by the T atom, the second column shows the number of Fe atoms within the sphere centered at the T atom and with radius of 2.7 Å. Note that $\Phi_{Fe-T}(r) > \Phi_{Fe-Fe}(r)$ in this range, more the Fe atoms in this range the more it is energy unfavorable, so there is a negative sign. The third column shows the number of Fe atoms within the range of 2.7–4.4 Å. Here $\Phi_{Fe-T}(r) < \Phi_{Fe-Fe}(r)$, more Fe atoms in this range the more it is energy favorable, so there is a positive sign. The fourth column shows the number of Sm atoms. Because $\Phi_{Sm-T}(r) > \Phi_{Sm-Fe}(r)$, it is unfavorable for energy

Table 6
Affecting factors vs. T atoms occupation sites

Site	Fe ($r<2.7$ Å)	Fe (2.7 Å $<r<4.4$ Å)	Sm	Total amount
8i	−7	+24	−1	$-7+24-1=16$
8j	−10	+19	−2	$-10+19-2=7$
8f	−11	+16	−2	$-11+16-2=3$

decrease, so a negative sign. From Table 6, it is easy to obtain the preferential occupation sequence, 8i > 8j > 8f.

5. Conclusion and discussion

The present work gives a series of interatomic pair potentials by using a number-theoretic lattice inversion formula based on ab initio cohesive energy calculation for selected simple virtual lattices. These quasi-ab initio interatomic potentials are used for the calculation of cohesive energy for a series of complex real Fe-based rare-earth compounds including the metastable phase $SmFe_{12}$, then phase stability, site preference, lattice parameters, possible space group and so on are evaluated at an atomistic level. In this work, a variety of samples for certain compositions with relaxed structures is taken into account. The interaction between distinct atoms A and B is calculated by an A–B system, not by combination of two pure element systems. All of these are different from Girt and Aitounian's successful method [16–18]. The calculated results in the present work are in unexpectedly good agreement with the experiment.

(1) The calculation results show that when a small amount of ternary element T (T = Cr, Mo, Ti and V) is added, the cohesive energy of $Sm(Fe,T)_{12}$ decreases, and its space group keeps I4/mmm unchanged, demonstrating that these elements can stabilize the structure of $ThMn_{12}$.
(2) When the ternary element is Mn, $\Phi_{Fe-T}(r) < \Phi_{Fe-Fe}(r)$ and $\Phi_{T-T}(r) < \Phi_{Fe-Fe}(r)$, in a wide range, the convex shape of the energy ~ content curve shows that the energy decreases drastically as the Mn content is great. Therefore, different from $SmFe_{12}$, the $SmMn_{12}$ is a stable binary phase with the structure of $ThMn_{12}$.
(3) As the T (T = Cr, Mo, Ti and V) atoms substitute Fe atoms at 8i sites, the crystal cohesive energy decreases most significantly, as the T atoms substitute Fe atoms at 8j sites the energy decrease is weak, as the T atoms substitute Fe atoms at 8f sites the energy decrease is the least. Therefore, the T atoms preferentially occupy 8i sites.
(4) The crystal structure obtained from the calculation maintains I4/mmm space group to a certain extent through overall deformation, a random atomic motion in the range of 0.6 Å and relaxation under the control of interatomic pair potentials. The initial structure has a randomness to a certain extent but the final structure is stable. All of these verify that the interatomic pair potentials based on the lattice inversion is effective to a certain extent.
(5) Through molecular dynamic simulation at different temperatures or sample random selection from numerous equilibrium samples at a certain temperature, the crystal structure maintains I4/mmm space group to a certain extent and the lattice constants approximately coincide with the experimental data. Additionally, the space group tolerances at different temperatures are approximately equal to the corresponding mean square root displacements. These facts further verify that the interatomic pair potentials based on the lattice inversion are effective, fully demonstrating that the pair potentials obtained from the inversion of first principle cohesive energy curve not only reflect the characteristics of

ideal equilibrium crystals but also partly reflect the characteristics of non-equilibrium crystals.

(6) How does the ternary element stabilize the crystal structure? To study this problem, more factors should be considered, such as solubility. Fig. 4 shows that as the substitution ternary element content exceeds a certain value, the energy rises again, that means the solubility is limited. Actually, as T = Ti, the limited solubility $x = 1$, as T = Cr or Mn, the limited solubility is $x = 2$, as T = V the limited solubility range is $1.4 < x < 3.5$ [4]. These phenomena cannot be explained self-consistently and perfectly only by the energy curves The entropy and the three-body potentials have to be studied, that will be our next objectives.

(7) All of these positive results have been extended to evaluate the structural properties for the emerging Fe-based rare-earth compounds such as $R(Fe,T)_{12}$, $R_2(Fe,T)_{17}$ and $R_3(Fe,T)_{29}$ [19], the systematic researches encourage us to predict some new materials with new structures in further study. Also, it might provide some new challenges for calculating the solubility of additional atoms. A further improvement of interatomic potentials might be necessary for extensive applications.

Acknowledgements

The authors would like to express their deep gratitude to the referee and editor of JMMM for their helpful suggestions. The present work was supported partially by National Foundation of Sciences in China, partially by National Advanced Materials Committee of China.

References

[1] Y.C. Yang, B. Kebe, W.J. James, J. Appl. Phys. 52 (3) (1981) 2077.
[2] D.B. deMooij, K.H.J. Buschow, Philips J. Res. 42 (1987) 246.
[3] F.R.de. Boer, H. Ying-kai, D.B. Mooij, K.H.J. Buschow, J. Less-Common Met. 135 (1987) 199.
[4] K.H.J. Buschow, J. Appl. Phys. 63 (8) (1988) 3130.
[5] R.B. Helmholdt, J.J.M. Vleggaar, K.H.J. Buschow, J. Less-Common Met. 138 (1988) L11.
[6] K. Ohashi, Y. Tawara, R. Osugi, M. Shimao, J. Appl. Phys. 64 (10) (1988) 5714.
[7] C.S. Kim, S.Y. An, Y.R. Uhm, S.W. Lee, Y.B. Kim, J. Appl. Phys. 83 (11) (1998) 6929.
[8] C.-K. Loong, S.M. Short, J. Lin, Y. Ding, J. Appl. Phys. 83 (11) (1998) 6926.
[9] N.X. Chen, Z.D. Chen, Phys. Rev. B 57 (1998) 14203.
[10] N.X. Chen, G.B. Ren, Phys. Rev. B 45 (1992) 8177.
[11] N.X. Chen, X.J. Ge, Phys. Rev. B 57 (1997) 14203.
[12] J. Maddox, Nature 344 (1990) 377.
[13] W.Q. Zhang, Q. Xie, X.J. Ge, N.X. Chen, J. Appl. Phys. 82 (2) (1997) 578.
[14] X.J. Ge, N.X. Chen, J. Appl. Phys. 85 (7) (1999) 3488.
[15] J. Hu, T. Wang, S.G. Zhang, Y.Z. Wang, J. Magn. Magn. Mater. 74 (1988) 22.
[16] E. Girt, Z. Altounian, D.H. Ryan, JMMM177-181, (1998) 982.
[17] E. Girt, Z. Altounian, Phys. Rev. B 57 (1998) 5711.
[18] E. Girt, Z. Altounian, J. Appl. Phys. 87 (1998) 4747.
[19] N.X.Chen, unpublished.